Macromolecules

ARTICLE

pubs.acs.org/Macromolecules

Hierarchical Organometallic Materials: Self-Assembly of Organic−Organometallic Polyferrocenylsilane Block Polyelectrolyte−Surfactant Complexes in Bulk and in Thin Films

Rumman Ahmed, Sanjib K. Patra, Laurent Chabanne, Charl F. J. Faul,* and Ian Manners*

School of Chemistry, University of Bristol, Cantock's Close, Bristol BS8 1TS, U.K.

Supporting Information

ABSTRACT: The self-assembly of well-defined organic−organometallic polystyrene-*b*-poly(ferrocenylmethyl(dimethylaminopropynylsilane)) (PS-*b*-PFAMS) diblock copolymers has been systematically investigated by varying the volume fraction of the organometallic block (PFAMS). Quaternization of the PFAMS block yielded PS-*b*-*q*PFAMS, which was ionically complexed to the anionic surfactants sodium bis(2-ethylhexyl) sulfosuccinate (AOT) and sodium bis(2,2,3,3,4,4,5,5,5-nonafluoropentyl) sulfosuccinate (AOT_F). The self-assembly of the block copolymer-surfactant complexes was also studied in bulk and thin films and produced materials with structural hierarchy over multiple length scales as shown by AFM, TEM, and SAXS studies.

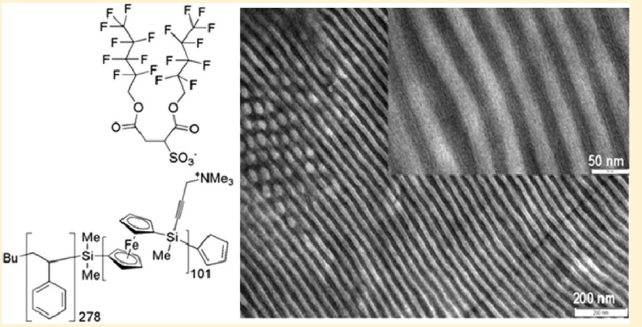

INTRODUCTION

The bulk state self-assembly of block copolymers forms periodic, phase-separated arrays of nanostructures with morphological characteristics that depend on the relative lengths of the blocks, the molecular weight, and the Flory−Huggins interaction parameter χ.[1] As a result of the periodic length scales (typically 10−100 nm), self-assembled block copolymers are promising candidates for applications in nanoscience. For example, ordered thin films of block copolymers can be used to fabricate high-density arrays for microfiltration, data storage, and photonics applications.[2] For example, films consisting of domains of perpendicularly oriented cylinders have been extensively investigated.[3] The combination of block copolymer self-assembly with supramolecular interactions can yield complex structures including aperiodic patterns. Selective addition of low molecular weight amphiphiles (of different nature and size) to one of the blocks using noncovalent interactions can add structural hierarchy and result in ordering over different length scales. Pioneered and developed by Ikkala and ten Brinke,[4] these systems have been extensively studied as a route to functional nanomaterials,[5] especially as this route shows promise for use in applications with switchable functionality.[6]

High molecular weight metal-containing polymers with well-defined and controlled architectures offer the prospect of additional functionality. Such materials have become of growing interest as a result of their interesting physical and chemical properties that offer a variety of potential applications.[7] For example, polyferrocenylsilanes (PFSs) (Chart 1), a class of metallopolymers,[8] have been shown to exhibit controlled responses to redox-stimuli,[9] etch resistance to plasmas,[10] and high refractive indices[11] and to function as precursors to nanostructured magnetic ceramics[12] and carbon nanotube growth catalysts.[13] Recent work has also focused on their ability to form crystalline, self-assembled materials.[14] Much research has been directed toward these metal-containing polymers as the iron moiety within the main chain offers access to a number of interesting properties.[8] As a result, several groups have studied the solid-state self-assembly of PFS block copolymers resulting in phase-separated iron-rich nanodomains.[15]

Chart 1. Structures of PFS and the Sila[1]ferrocenophane Monomer, fcSiMe(C≡CCH$_2$NMe$_2$)

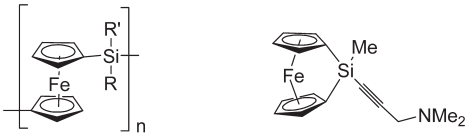

PFS 1

The most studied route to PFS block copolymers involves the use of sequential living anionic polymerization protocols with highly basic alkyl or aryl lithium reagents as initiators.[16] This process proceeds via cleavage of the Si-Cp (Cp = cyclopentadienyl) bond in the sila[1]ferrocenophane monomer. However, because of the highly basic nature of the anionic initiator and propagating center, many functional sila[1]ferrocenophane

Received: July 4, 2011
Revised: September 27, 2011
Published: November 15, 2011

Chart 2. Structures of the PS-*b*-qPFAMS Diblock Copolymer after Quaternization by Me_2SO_4, AOT (2), and AOT_F (3) Surfactants

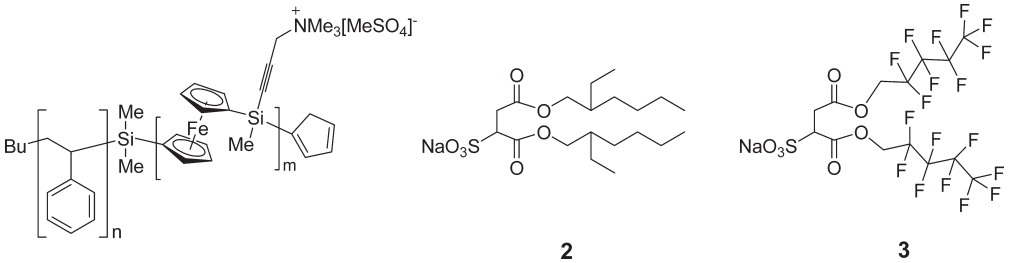

monomers such as fcSiMe(C≡CCH$_2$NMe$_2$) (**1**) (Chart 1) cannot be used due to side reactions at the acetylene group.[17]

Recently, an alternative photocontrolled living anionic polymerization method has been developed that involves photoactivation and subsequent cleavage of the iron−cyclopentadienyl (Fe−Cp) bond in the monomer in the presence of mild nucleophiles such as Na[C_5H_5] (NaCp).[18] This milder photolytic ring-opening polymerization (ROP) route therefore provides an attractive alternative for the synthesis of acetylene-functionalized PFS-containing diblock copolymers (which are readily further functionalized[17]) as well as cyclic polymers[19] and block copolymers containing different metals,[20] which are inaccessible via other routes.

To date, the only supramolecular approach employed to construct organized liquid-crystalline PFS nanomaterials (PFS polymers with pendant mesogenic side chains) has been achieved via the complexation of PFS polyelectrolytes to oppositely charged surfactants using the so-called ionic self-assembly (ISA) method.[21] However, the complexation of charged PFS diblock copolymers to oppositely charged surfactants (to yield hierarchically self-assembled nanostructures) has been left virtually unexplored. In this paper, we report the first example of hierarchical organic−organometallic materials prepared from charged PFS diblock copolymers using this powerful ISA method.[22] This was achieved by complexation of quaternized polystyrene-*b*-poly(ferrocenylmethyl(dimethylaminopropynylsilane)) (PS-*b*-*q*PFAMS) (Chart 2) with the anionic surfactants sodium bis(2-ethylhexyl) sulfosuccinate (AOT), **2**, or sodium bis(2,2,3,3,4,4,5,5,5-nonafluoropentyl) sulfosuccinate (AOT_F), **3**.

A potential advantage of having an organic block in conjunction with PFS within the structural hierarchy is the ability to use the organic block as a sacrificial template element. This strategy offers the possibility for post self-assembly modifications, such as selective etching and lithography, to yield organized inorganic nanostructures as a result of the higher etch resistance of the PFS block.[10,23]

■ RESULTS AND DISCUSSION

Synthesis and Characterization of the PS-*b*-PFAMS Diblock Copolymers 4−6. First, the desired PS-*b*-PFAMS block copolymers **4**−**6** were prepared using a recently reported strategy that combines the living anionic polymerization of styrene and the photocontrolled living polymerization of sila[1]ferrocenophanes.[24] *sec*-BuLi was used to initiate anionic polymerization of styrene using cyclohexane as the solvent. The living polystyrene was then quenched with excess dichlorodimethylsilane and the subsequent reaction with $MgCp_2$ yielded the Cp-end-capped polystyrene (PS-Cp). The PS-Cp was then used to macroinitiate amino-functionalized sila[1]ferrocenophane (**1**)

Scheme 1. Synthesis of the PS-*b*-PFAMS Diblock Copolymers 4−6

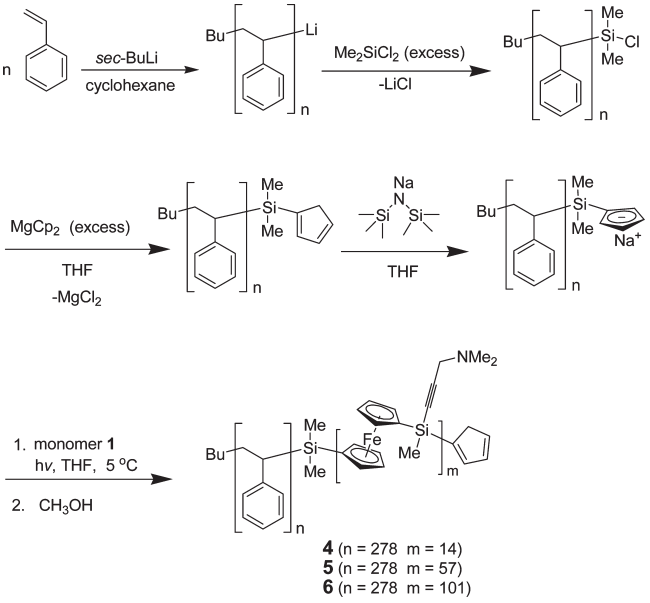

through photolytic ROP, after the deprotonation of the end-capped Cp using sodium bis(trimethylsilyl)amide as shown in Scheme 1.

This milder photocontrolled anionic polymerization using the moderately basic Cp anion-based macroinitiator yielded the desired PS-*b*-PFAMS diblock copolymers with controlled molecular weight and narrow polydispersities. Three different PS-*b*-PFAMS diblock copolymers were synthesized in this study with the aim of obtaining specific morphologies (spheres, cylinders, and lamellar; *vide infra*) within the phase diagram[25] of linear AB block copolymers (Table 1).

Both ^{1}H NMR and gel permeation chromatography (GPC) studies (using a triple detector GPC equipped with refractometer, viscometer, and light scattering detectors; see Experimental Section) allowed us to determine the overall molecular weight of the block copolymers. Figure 1 shows the GPC chromatogram of **6** and the corresponding polystyrene homopolymer. In addition, the ^{1}H NMR spectrum of **6** showed the relevant peaks corresponding to both of the blocks (Figure S1 in Supporting Information). GPC analysis (triple-detection) of an aliquot of the PS homopolymer obtained before the addition of the ferrocenophane monomer provided the absolute molecular weight of the first block. Using ^{1}H NMR integration, the overall polymer molecular weight was estimated by comparing the

Table 1. Characterization Data for PS-*b*-PFAMS Diblock Copolymers

polymers[a]	Φ_{PFAMS}[b]	M_n (g/mol)[c]	PDI[d]	yield (%)	predicted morphology
PS_{278}-*b*-$PFAMS_{14}$ (**4**)	0.11	33 240	1.09	84	spheres
PS_{278}-*b*-$PFAMS_{57}$ (**5**)	0.33	46 525	1.11	89	cylinders
PS_{278}-*b*-$PFAMS_{101}$ (**6**)	0.47	60 120	1.07	85	lamellar

[a] Subscripts denote degrees of polymerization with respect to each block; the block ratio was calculated using ^{1}H NMR integration. [b] Volume fractions of PFAMS were calculated considering the following density values (ρ) from the two blocks: PS = 1.0 kg/m^3, PFAMS[26] = 1.24 kg/m^3. [c] Molecular weight of the block copolymer, determined by combining the M_n of the PS block and the block ratio (obtained from ^{1}H NMR). [d] Determined from conventional salt-based GPC (using polystyrene standards, M_w/M_n), and THF containing 0.1 wt % ^{n}Bu$_4$NBr.

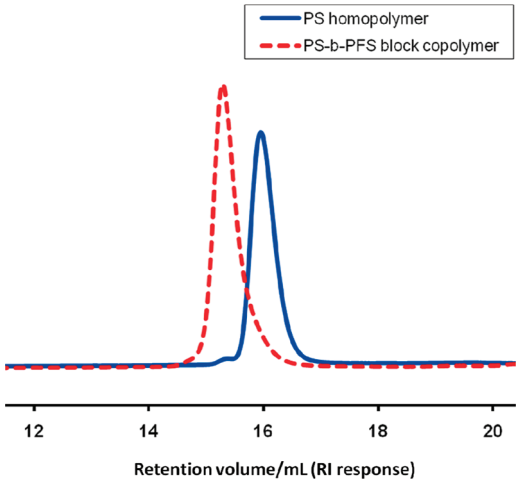

Figure 1. GPC chromatogram of the PS homopolymer (triple detection GPC using THF as eluent) and PS-*b*-PFAMS diblock copolymer **6** (GPC relative to polystyrene standards, using 0.1 wt % ^{n}BuN_4Br in THF as eluent).

integration of the NMe_2 protons (from PFAMS) in relation to the CH_2 protons (from PS). Furthermore, conventional calibration GPC (eluent: THF containing 0.1 wt % [Bu_4N]Br) relative to polystyrene standards[27] was used to determine the PDI of the PS-*b*-PFAMS diblock copolymers.

Synthesis of PS-*b*-qPFAMS Block Polyelectrolytes 7−9 and Their Surfactant Complexes. The diblock copolymers **4**−**6** were quaternized using dimethyl sulfate[17] to yield block polyelectrolytes **7**−**9**, as shown in Scheme 2. These polyelectrolytes were characterized readily using ^{1}H NMR spectroscopy, which clearly indicated the successful conversion of the dimethyl amine groups into the trimethylammonium moieties (see Figure S1 for ^{1}H NMR). For example, the methyl protons of the ammonium group in **9** exhibited a signal at δ = 2.59 ppm, which was shifted significantly downfield from the dimethylamino protons in the block copolymer **6** (δ = 2.34 ppm) as a result of the quaternization. Furthermore, the methylene protons (adjacent to the nitrogen atom) exhibited a downfield shift from 3.38 ppm in block copolymer **6** to 3.50 ppm in the block polyelectrolyte **9**. In addition, the absence of residual dimethylamino proton signals in the ^{1}H NMR spectrum of **9** confirmed that the quaternization had proceeded to ca. 100% completion.

Next, these block polyelectrolytes were complexed with oppositely charged surfactants **2** and **3** in a 1:1 charge stoichiometry. Complexations were performed by dissolving both building blocks separately in deionized water (1 wt %, 70 °C). After complete dissolution, the surfactant solution was added dropwise to the block polyelectrolyte solution. Once isolated, the charge-neutralized complexes were readily soluble in common organic solvents such as chloroform, THF, and toluene.

Self-Assembly of PS-*b*-PFAMS Diblock Copolymers 4−6 in the Bulk and Thin Films. Prior to studying the self-organization of the block polyelectrolyte−surfactant complexes, the self-assembly of the diblock copolymers was investigated to gain insight into their morphologies both in bulk and in thin films. For self-assembly in the bulk, films of PS-*b*-PFAMS (**4**−**6**) were prepared by allowing the solvent (toluene) to evaporate slowly from a concentrated solution of the copolymer (50 mg/mL) cast on a glass slide. The films were then dried at 50 °C overnight in a vacuum oven and further annealed at ca. 130 °C under vacuum (1×10^{-2} mmHg) for 5 days. To study the morphology of the thermally annealed films by transmission electron microscopy (TEM), ultrathin sections were prepared by room temperature microtoming of samples mounted on an epoxy resin using cyanoacrylate glue. The bright-field TEM images of the unstained sections of **4**−**6** are shown in Figure 2d−f. The high electron density of the Fe-containing PFAMS block provides sufficient contrast for TEM imaging without staining, and we assign the dark domains to be PFS and the lighter to be PS. As predicted, the diblock copolymers **4**−**6** with volume fractions of PFAMS (Φ_{PFAMS}) of 0.11, 0.33, 0.47 (see Table 1) formed spherical, cylindrical, and lamellar morphologies, respectively. Some small cylinders were present among the spheres in Figure 2d, indicating that **4** (Φ_{PFAMS} = 0.11) may be close to the phase boundary. The bulk thermally annealed self-assembled diblock copolymers were further analyzed using small-angle X-ray scattering (SAXS) (Figure 2a−c). The corresponding reflections for **4**−**6** obtained by SAXS provided complementary support for the morphologies observed by TEM. Furthermore, the average *d*-spacing observed from the SAXS reflections correspond to the periodicities observed from TEM studies. The *q* ratios detected for **4**, **5**, and **6** were consistent with spheres, hexagonal ordered arrays of cylinders, and a lamellar morphology, respectively. The thin-film self-assembly of the diblock copolymers **4**−**6** was investigated using atomic force microscopy (AFM). Solutions of the diblock copolymers in toluene (10 mg/mL) were spin-coated onto silicon substrates and further annealed in saturated toluene vapor overnight. The organic PS block was then selectively removed using an oxygen plasma leaving behind an etch resistant iron/silicon oxide layer, which preserved the PFS domains.[10d] Tapping mode AFM of the thin films showed the corresponding morphologies of spheres, cylinders, and lamellae respectively (Figure 2g−i).

Hierarchical Structures upon Complexation with Anionic Surfactants. Self-assembly of block copolymers takes place on a length scale of 10−100 nm, whereas self-assembly between the polymer−amphiphile (as a result of ISA) takes place between 2 and 3 nm. Therefore, a combination of these two processes,

Scheme 2. Quaternization of Diblock Copolymers 4−6 to Obtain the Respective Block Polyelectrolytes 7−9 and the Consequent Complexations with Anionic Surfactants

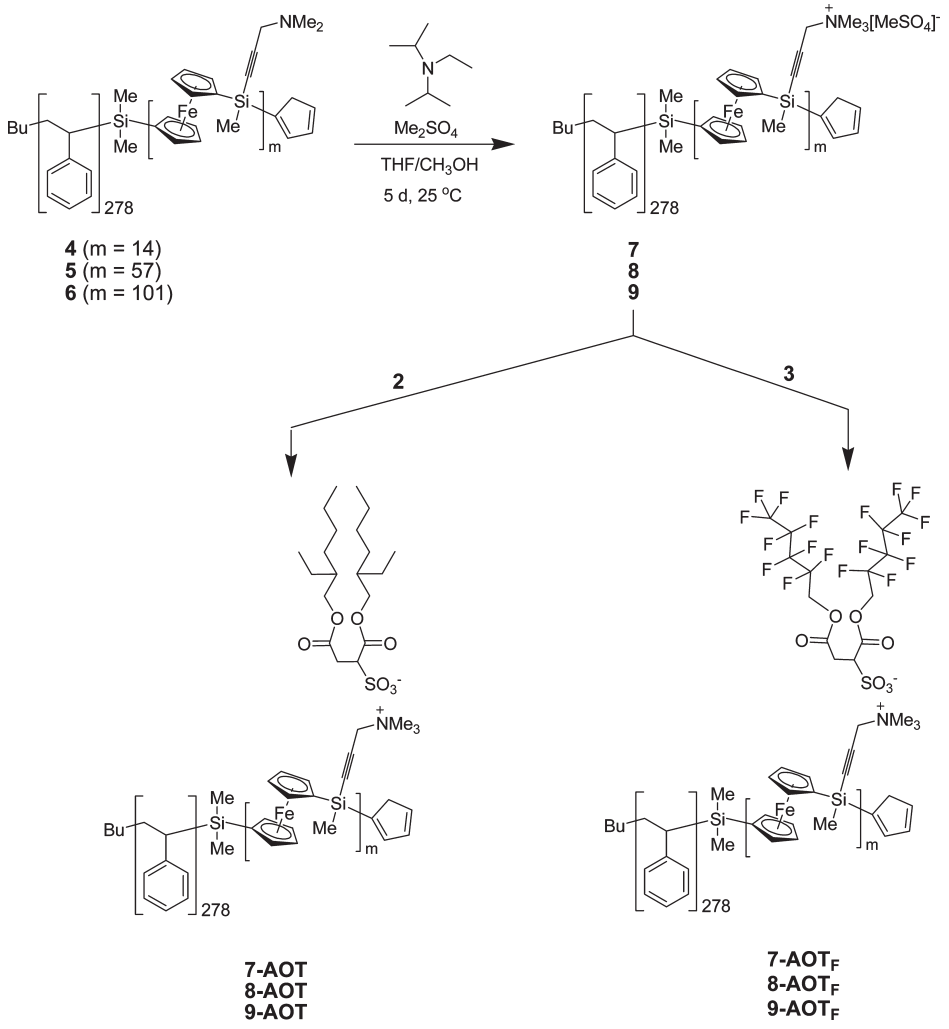

which involve competing interactions at different length scales, should lead to hierarchical architectures, as shown in Scheme 3.

*Self-Assembled Structures from **7-AOT**, **8-AOT**, and **9-AOT**.* Figure 3 shows the morphology obtained from the ISA material **7-AOT**. The thin film morphology of the complex was investigated using tapping mode AFM. These films were prepared by spin-coating the material from solution (toluene, 10 mg/mL) followed by annealing in saturated toluene atmosphere overnight. The observed cylindrical morphology (Figure 3a) was expected for **7-AOT** as a result of the surfactant's mass increasing the overall volume fraction of the PFAMS block from Φ_{PFAMS} = 0.11. According to the classical phase diagram for block copolymers,[25] this would move the expected morphology into the area of cylinders. SAXS studies of the bulk annealed complex (Figure 3b) supported the formation of a hexagonal phase at the block copolymer length scale (reflections in the ratio of 1:$\sqrt{3}$), which complemented the morphology information from AFM and TEM. Furthermore, a broad reflection at higher q values was observed (q = 2.7 nm^{-1}) corresponding to an average d-spacing of 2.3 nm, which can be attributed to a periodic structure originating from the phase-separated PFAMS−AOT block as a result of ISA. SAXS analyses, in conjunction with AFM and TEM investigations, provided evidence for the hierarchical organization of **7-AOT** at different length scales.

High-temperature annealing (ca. 130 °C) of the bulk material **7-AOT** above its T_g (ca. 101 °C, obtained from differential scanning calorimetry, DSC), followed by microtoming thin sections (ca. 60 nm) for TEM analysis, yielded images of cylindrical domains distorted in certain regions, as shown in the TEM micrograph (Figure 3e). These distortions can result from microtoming effects whereby cutting thin slices of the annealed material with a diamond tip can lead to deformations. In addition, mixing between the alkyl tails of the surfactant and the polystyrene can take place at elevated temperatures. This phenomenon has been investigated previously by Ikkala and Faul et al.,[28] where shear alignment of ordered perylene-based ISA nanomaterials was enabled through compatibilization of the perylene phase with the bulk PS through the ionically attached branched surfactant tails. In our complexes it is postulated that a certain degree of mixing can take place between the polystyrene block and the AOT surfactants at elevated temperatures, resulting in a distorted hexagonal packing. DSC (Figure 4) provided further insight into the mixing behavior of the PS block with the alkyl tails. Instead of two separate signals for the glass

dx.doi.org/10.1021/ma201526w |*Macromolecules* 2011, 44, 9324–9334

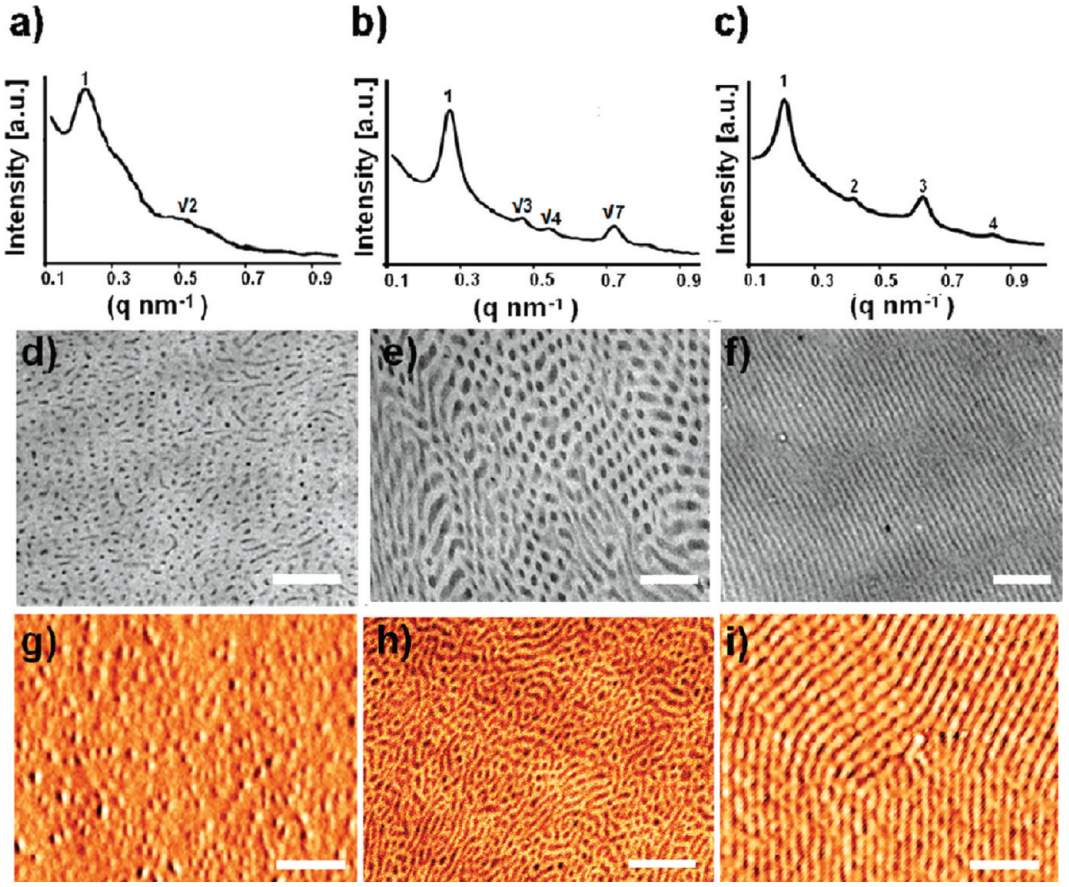

Figure 2. SAXS reflections of the bulk self-assembled diblock copolymers: (a) **4** (Φ_{PFAMS} 0.11); (b) **5** (Φ_{PFAMS} 0.33); (c) **6** (Φ_{PFAMS} 0.47). Bright-field TEM images of (d) **4**, (e) **5**, and (f) **6** (scale bar = 200 nm). Tapping mode AFM phase images of the diblock copolymer thin films after oxygen plasma etching (substrate = silicon, tip = Si_3N_4): (g) **4**, (h) **5**, and (i) **6** (scale bar = 200 nm).

Scheme 3. Schematic Representation of the Formation of Hierarchically Self-Assembled Architectures, Illustrating the Concept of Structure-within-Structure Formation

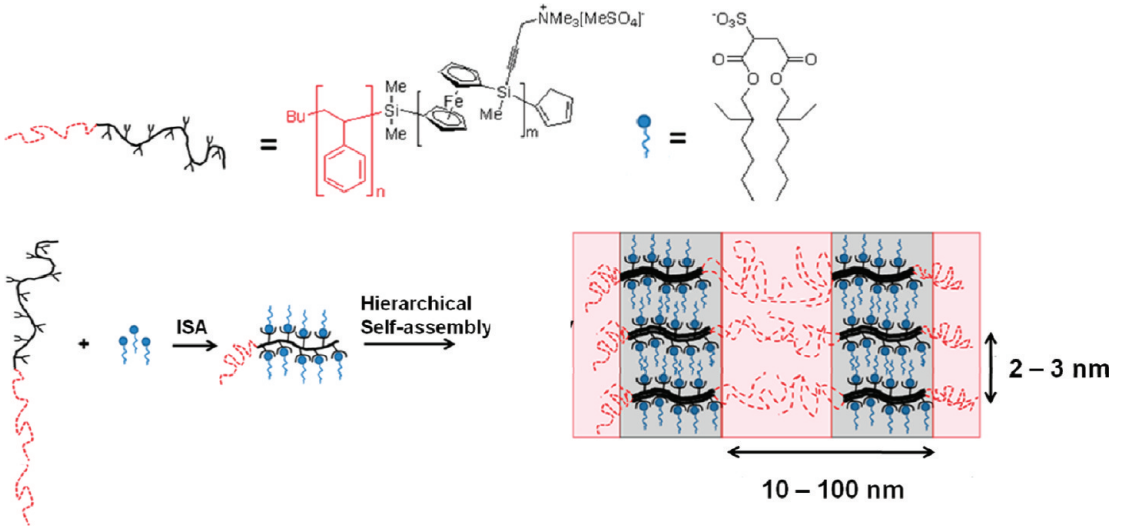

transition temperatures (T_g) corresponding to the two blocks in the complex, only one T_g was observed, thus indicating the miscibility of the two blocks. The first heating cycle (solid line) showed a T_g at 101 °C, corresponding to the PS block. Above this temperature, it is expected that the alkyl tails start to mix with the PS segment. This can be clearly seen in the second heating cycle

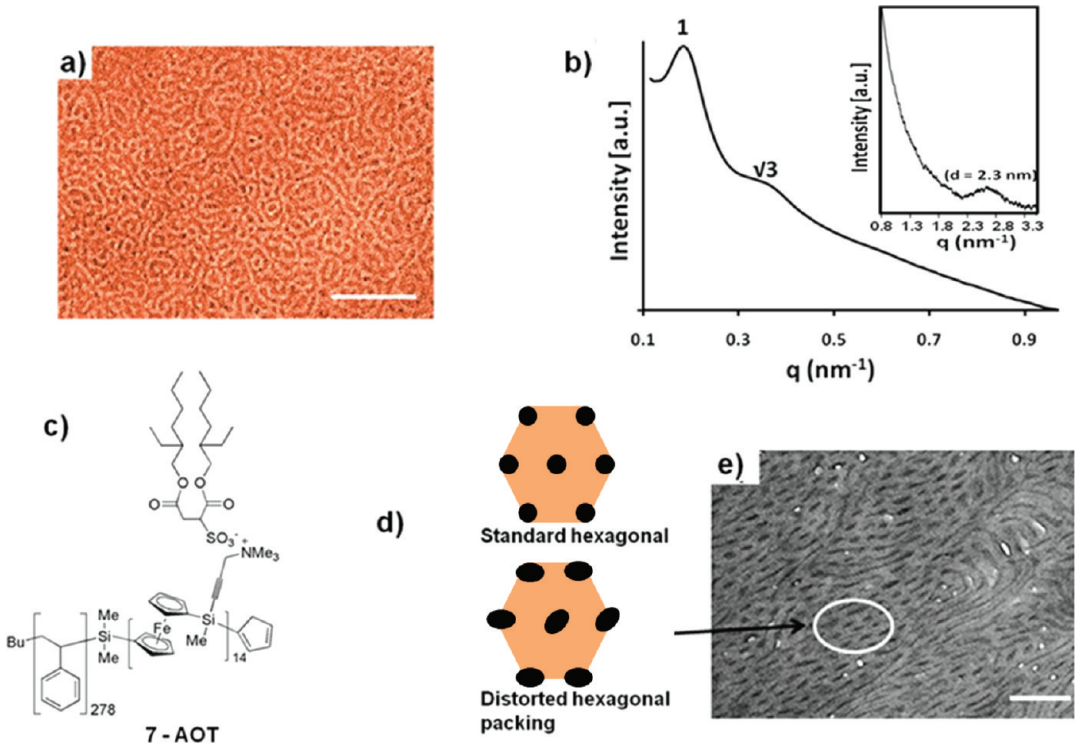

Figure 3. Morphological characterization of **7-AOT**. (a) Tapping mode AFM phase image, spin-coated onto silicon from 1 mg/mL toluene using a Si_3N_4 tip (scale bar = 500 nm). (b) SAXS reflections at the small and larger q values. (c) Structure of the complex. (d) Cartoon representing the distortion effect of microtoming. (e) TEM micrograph of microtomed sections (60 nm) (annealed for 5 days at 130 °C) (scale bar = 200 nm).

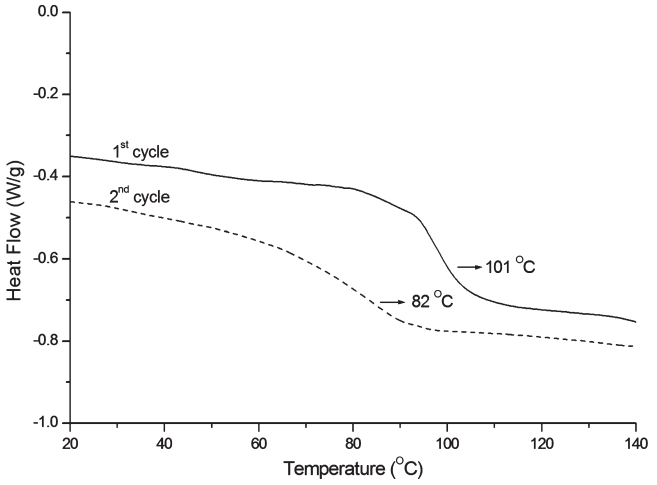

Figure 4. DSC of **7-AOT** (heating rate: 10 °C/min) showing the reduced T_g of the complex with increased plasticization by the surfactant alkyl tails.

(dotted line), where the T_g (for the PS block) is reduced to 82 °C as a result of plasticization.[29]

Complexation of **8** and **9** with AOT showed similar results to **7-AOT**. Figure 5a illustrates the corresponding AFM phase image of **9-AOT**, showing a cylindrical morphology. Once again, this morphology was expected, as the calculated volume fraction (with respect the PFAMS block) increases from Φ_{PFAMS} 0.47 upon complexation with the amphiphile. Analogous to the results observed for **7-AOT**, high-temperature annealing (ca. 130 °C, 5 days) of **9-AOT** resulted in distorted lamellar morphologies, as observed from the TEM micrograph (Figure 5d). It is proposed that the presence of additional AOT units along the PFAMS backbone provides a higher degree of mixing with the PS at elevated temperatures, resulting in a distorted lamellar morphology. SAXS analysis (at low q values) of the bulk annealed complex resulted in a broad first-order reflection observed at $q = 0.22$ nm^{-1}, corresponding to a d-spacing of 29 nm. Additional weak reflections were also observed, however, the ratios could not be indexed to a particular morphology. This was consistent with observations seen for TEM analysis whereby no definitive morphology was observed. SAXS at higher q values yielded a broad reflection with average d-spacing of 2.5 nm, indicative of organization at the polymer−surfactant length scale as a result of ISA.

It should also be noted that using this supramolecular approach, we were able to obtain hierarchical morphologies which would otherwise be extremely difficult to obtain with diblock copolymers. However, from an applications perspective, this mixing behavior between the alkyl tails and the PS is not ideal. The distorted morphologies observed for **7-AOT** and **9-AOT** would be of no benefit in terms of templating and/or material fabrication where organized architectures over large length scales are essential. In order to test our hypothesis (and at the same time to circumvent these problems), we decided to introduce fluorocarbon units within the surfactant tails and complex the quaternized block copolymers with $\mathbf{AOT_F}$. This strategy would prevent any mixing between the surfactant tails and the PS at high temperatures, owing to the highly hydrophobic nature of fluorocarbons.[30] Furthermore, the presence of fluorine in the PFAMS block will also facilitate greater segregation behavior between the two blocks in such systems by increasing the Flory−Huggins parameter (χ) between the two

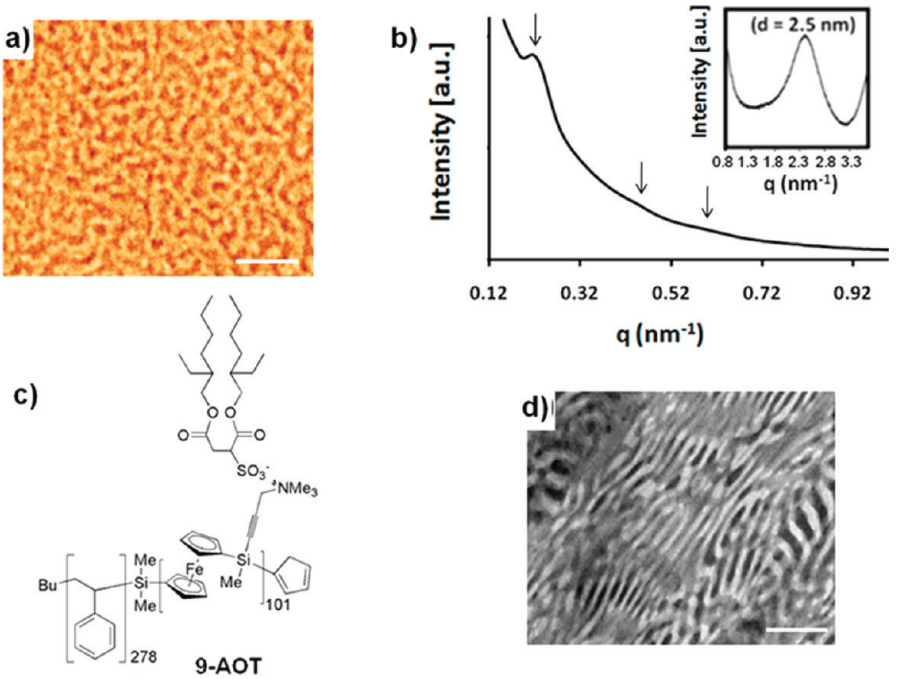

Figure 5. Morphological characterization of **9-AOT.** (a) AFM phase profile (spin-coated onto silicon from 1 mg/mL toluene using a Si_3N_4 tip); scale bar = 200 nm. (b) SAXS scattering of the sample. (c) Structure of the complex. (d) TEM micrograph of microtomed sections (60 nm), annealed for 5 days at 130 °C (scale bar = 200 nm).

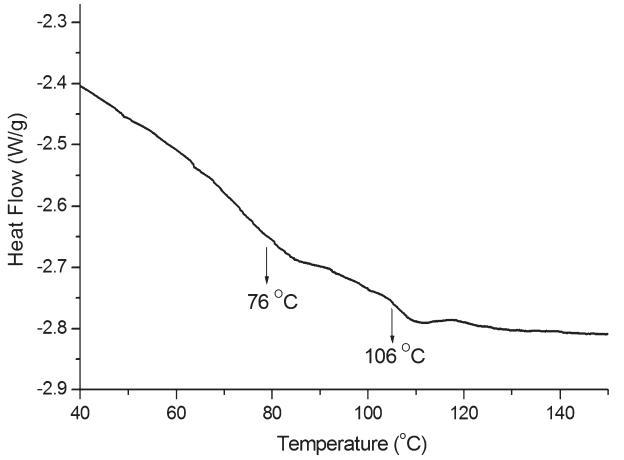

Figure 6. DSC thermogram for **9-AOT$_F$** (heating rate: 10 °C/min) showing two distinct T_g's.

different blocks (as a result of a larger difference in the corresponding solubility parameters[31]). Numerous articles have been published by Thünemann et al.[32] on the preparation of thin films with ultralow surface energies as a result of the complexation of polyelectrolytes with a range of oppositely charged fluorinated surfactants.

*Self-Assembly of **7-AOT$_F$**, **8-AOT$_F$**, and **9-AOT$_F$**.* Unlike **7-AOT**, **8-AOT**, and **9-AOT**, DSC measurements of **7-AOT$_F$**, **8-AOT$_F$**, and **9-AOT$_F$** showed two distinctive endothermic transitions. For example, the DSC thermogram for **9-AOT$_F$** showed a T_g centered at 106 °C (for the PS block) and 76 °C (for the PFAMS-AOT$_F$ block), as shown in Figure 6. The glass transition temperatures obtained were consistent with those of the corresponding homopolymers (see Figure S2). The presence of two distinct glass transition temperatures (which are close in value to the individual homopolymers) indicated the immiscibility between the blocks.

The bulk and thin film self-assembly of both **7-AOT$_F$** and **8-AOT$_F$** displayed spherical and lamellar morphologies, respectively (see Figures S3 and S4). Figure 7 shows the morphological characterizations of the complex **9-AOT$_F$**. TEM analysis (Figure 7b) of the thermally annealed complex (ca. 130 °C, 5 days) presented well-defined polystyrene cylinders within a PFAMS−surfactant matrix with average periodicities of 35 nm. The highly hydrophobic fluorocarbon groups clearly introduce a much stronger segregation between the PS and the fluorocarbon-containing PFAMS blocks, resulting in an increase in χ and thus sharper phase boundaries at the interface between the blocks. Furthermore, thermal annealing has resulted in relatively well-aligned cylinders spanning over several micrometres in length. SAXS was also performed on the thermally annealed self-assembled complex (Figure 7c). The reflections observed at the block copolymer length scale were consistent with that of a hexagonal phase.[33] In addition, scattering at larger q values depicted a broad reflection at q = 2.6 nm^{-1} (d = 2.4 nm), indicative of ordering at the polymer−surfactant length scale as a result of ISA. However, the nature of the poor scattering prevented full structural assignment of materials at the surfactant length scale. Nevertheless, SAXS data along with the TEM/AFM characterization clearly illustrated hierarchical organization at two different length scales. Thin films of the complex were investigated using tapping mode AFM (Figure 7d) (obtained by spin-coating **9-AOT$_F$** (toluene, 10 mg/mL) and annealing in a saturated toluene atmosphere overnight). These films (ca. 50 nm thick) were then etched under an oxygen plasma to selectively remove the organic components, thus leaving behind a ceramic residue derived from the etch-resistant PFAMS block. The AFM phase images were reminiscent of a hexagonal close packed array of

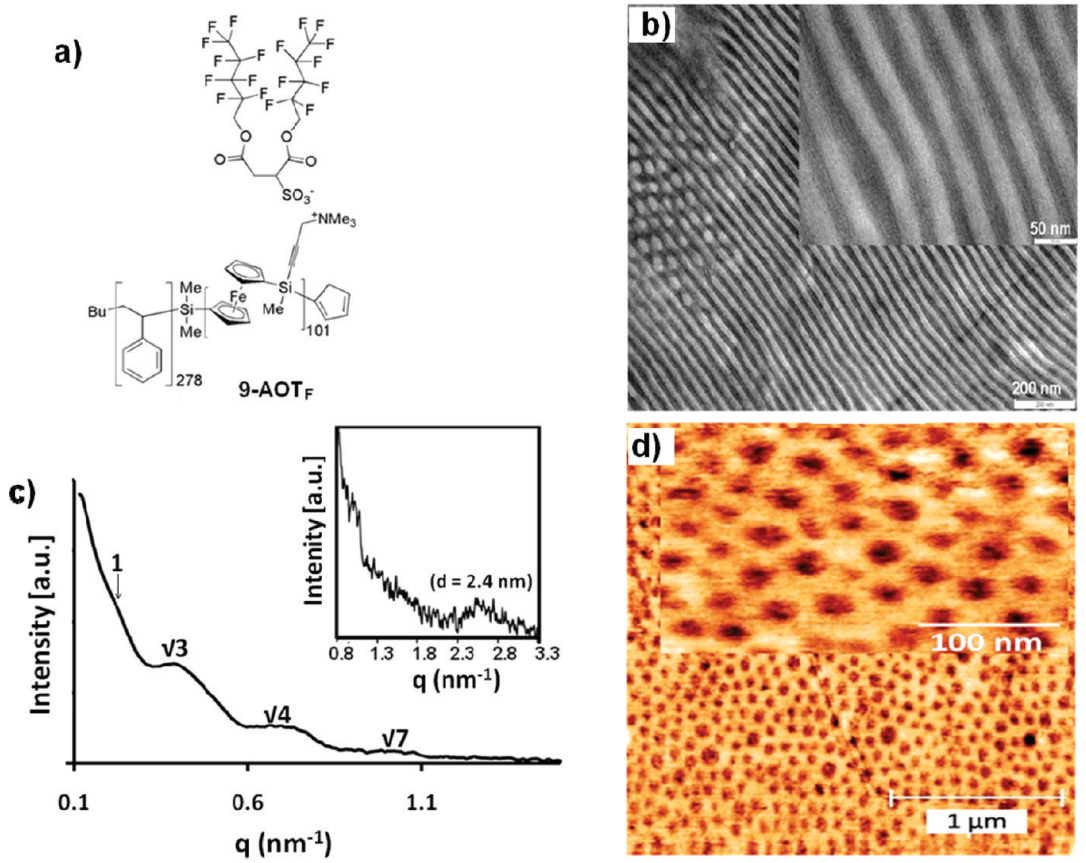

Figure 7. (a) Structure of the complex **9-AOT$_F$**. (b) TEM micrograph of microtomed sections at 60 nm. (c) SAXS patterns at small and large length scales. (d) AFM phase profile portraying the cylinders after etching the organic block with an oxygen plasma (tapping mode using a Si_3N_4 tip).

holes (as a result of the removal of the PS segments) with average periodicities of 34 nm.

CONCLUSIONS

We have demonstrated the first example of an organic—organometallic hierarchically organized nanostructure from the ionic complexation of PS-*b*-PFAMS diblock copolymer with low molecular weight amphiphilic molecules. Furthermore, we have shown that this method can provide a simple route to achieving multiple goals within one system, including hierarchical organization at different length scales, the generation of nanostructured materials, and inducing certain functionality by careful selection of starting materials. We have also demonstrated that fine structural tuning can be achieved by careful selection of the amphiphile for complexation. For example, in **9-AOT$_F$**, the presence of fluorocarbon segments resulted in material that phase separated into well-defined structures with sharp boundaries even at elevated temperature.

EXPERIMENTAL SECTION

Materials and Equipment. All chemicals were purchased from Aldrich unless otherwise noted. Trimethylchlorosilane (Me_3SiCl) and dichlorodimethylsilane (Me_2SiCl_2) were distilled prior to use. Solvents were dried using Anhydrous Engineering double alumina and alumina/copper catalyst drying columns or by conventional methods. Methanol, used for quenching the polymerization, was deoxygenated using the freeze and thaw method. Cyclohexane and THF were distilled under reduced pressure from *n*BuLi and Na/benzophenone, respectively, prior to each photolytic polymerization reaction. Styrene monomer was dried over CaH_2 for 24 h and subsequently distilled twice under reduced pressure prior to polymerization. All reactions and manipulations were carried out under an atmosphere of prepurified N_2 by using standard Schlenk techniques or an inert atmosphere glovebox (M-Braun) purged with prepurified Ar. The photoirradiation experiments were carried out using Pyrex-glass-filtered emission (λ > 310 nm) from a 125 W high-pressure Hg arc lamp (Photochemical Reactors Ltd.).

Monomer **1** [fcSiMe(C≡CCH$_2$NMe$_2$)] was prepared following previous literature[17] and was purified by repetitive crystallizations and sublimations to obtain spectroscopically pure material suitable for photolytic ring-opening polymerization (PROP). Magnesocene ($MgCp_2$) was prepared according to a literature-known procedure,[34] and it was sublimed twice before use. AOT$_F$ was synthesized following a previously reported literature procedure.[35] ^{1}H (300 MHz), ^{13}C {^{1}H} (75.4 MHz), and ^{19}F {^{1}H} (282.6 MHz) NMR spectra were obtained from Jeol Lambda 300 spectrometer. Solid-state FT-IR spectra (Bruker) were recorded in transmission mode on a quartz surface using a pressure-sensitive arm. Molecular weights of polymers and polydispersity indices (PDI = M_w/M_n) of all the PS homopolymers were obtained by gel permeation chromatography (GPC) using a Viscotek VE 2001 triple-detector gel permeation chromatograph equipped with automatic sampler, pump, injector, inline degasser, column oven (30 °C), styrene/divinylbenzene columns with pore sizes of 500 and 100 000 Å, VE 3580 refractometer, four-capillary differential viscometer, and 90° angle laser and low angle laser (7°) light scattering detector (VE 3210 and VE270). THF stabilized with 0.025% butylated hydroxytoluene (Fisher) was used as the

chromatography eluent, at a flow rate of 1.0 mL/min. Samples were dissolved in the eluent (2 mg/mL) and filtered (Acrodisc, PTFE membrane, 0.45 mm) before analysis. Calibration of all three detectors (refractive index, laser light scattering, and viscometry) was performed using polystyrene standards purchased from Viscotek. This equipment allows the exact measure of homopolymer molecular weights and PDIs. When conventional calibration was employed, molecular weights were determined relative to polystyrene standards purchased from Aldrich. For conventional calibration, the eluent contained 0.1 wt % $[Bu_4N]Br$. Differential scanning calorimetry (DSC) was performed on a TA Instruments DSC Q100 apparatus coupled to a refrigerated cooling system (RCS90). Both heating and cooling scans were performed at 10 °C/min under an N_2 atmosphere with the samples between 5 and 8 mg contained in standard aluminum pans. The samples were heated to 200 °C from 20 °C, cooled to 20 °C, and heated to 200 °C again. The cycle was repeated twice. Bulk samples were microtomed at room temperature using a RMC MTXL ultramicrotome and a diamond knife. Copper grids from Agar Scientific (mesh 400) were coated with carbon film. Transmission electron microscopy (TEM) was performed on a Jeol 1200EX TEM Mk2, which operates with a tungsten filament operated at 120 kV. It is fitted with a MegaViewII digital camera, using Soft Imaging Systems GmbH analySIS 3.0 image analysis software. A Laurell WS-400B-6NPP/lite spin coater was used to prepare thin films which were subsequently plasma etched using a Harrick Plasma Cleaner. Thin film surface morphology of samples was assessed by scanning force microscopy (SFM) in both the height and phase modes using a Digital Instruments Nanoscope 3D AFM. SAXS was performed at the European Synchotron Research Facility (Grenoble, France).

Synthesis of Cp-Capped Polystyrene. Cp-capped polystyrene was synthesized as developed recently by our group.[24] Styrene (10.0 g, 96.15 mmol) was dissolved in cyclohexane (20 mL) and initiated with 255 μL of *sec*-Buli (1.4 M solution in cyclohexane) at ambient temperature in an inert atmosphere glovebox. The colorless solution turned orange instantaneously, indicative of formation of living polystyrene anions. The polymerization was terminated with a large excess of dichlorodimethylsilane (10 mL) and left stirring overnight. Solvent and the excess silanes were removed and dried under vacuum overnight. The product was dissolved in THF (10 mL), $MgCp_2$ (0.10 g, 0.65 mmol) was added, and the solution was stirred for 10 h. 1 mL of Me_3SiCl was then added to the mixture, and the solution was left stirring for 1 h. All the volatile materials were removed under vacuum. The polymer was redissolved in THF, precipitated into hexane, and filtered. It was then further purified by precipitating twice from THF into methanol. Finally, the pure Cp-capped PS was dried in a vacuum oven (60 °C, for 24 h) and stored in a glovebox. Yield (9.0 g, 90%). ^{1}H NMR (400 MHz, C_6D_6): δ = 1.90−1.35 (br, CH_2), 1.90−2.70 (br, CH), 6.33−7.26 ppm (m, Ph). $^{13}C\{^1H\}$ NMR (400 MHz, C_6D_6): δ = 41.0 (CH), 44.0 (CH_2), 125.7, 127−128.5 ppm (Ph). GPC analysis (THF, triple detection): M_n = 2.89 × 10^4 Da, PDI = 1.01

Synthesis of PS-*b*-PFAMS Copolymers 4−6. A representative polymerization is described for the synthesis of PS_{278}-*b*-$PFAMS_{101}$ (**6**). Cp-capped polystyrene (0.50 g, 0.017 mmol) was dissolved in THF (1 mL), and sodium bis(trimethylsilyl)amide (4.76 mg, 0.026 mmol) was added. The solution was left to stir for 1 h. To that solution, **1** (0.32 g, 1.041 mmol) was added. The reaction mixture was irradiated for 3 h at 5 °C. Irradiation was then stopped, and the living polymer chain ends were quenched using dry degassed methanol. The diblock copolymer **6** was then isolated by selective precipitation from THF in methanol and was in the form of an orange gum. Block copolymer **6** was then dried in vacuum (40 °C, 1 × 10^{-2} mmHg); yield 0.69 g (85%). Conventional GPC analysis indicated a PDI of 1.07. (Integration ratio from NMR studies gave an overall molecular weight of 6.0 × 10^4 Da). ^{1}H NMR (400 MHz, D_8 THF): δ = 0.64 (s, $SiCH_3$), 1.52 (m, aliphatic PS), 1.92 (m, aliphatic PS), 2.34 (s, NMe_2), 3.38 (s, CH_2N), 4.14−4.40 (m, Cp), 7.33−7.79 (m, Ph). $^{13}C\{^1H\}$ NMR (400 MHz, C_6D_6): δ = −4.7 (Si−CH_3), 44.1 (N−CH_3), 48.9 (N−CH_2), 69.1 (*ipso*-C), 70.6, 70.8, 71.4, 71.9, 72.1, 72.5, 72.6, 73.5, 73.6, 73.8, 74.2 (Cp), 87.9 (SiC≡CCH_2), 103.2 (SiC≡CCH_2), 122.3, 126.6, 128.3, 128.4, 128.6, 128.9 (PS). GPC: homopolymer aliquot (PS) M_n = 2.89 × 10^4 Da and ^{1}H NMR integration ratio of 1:1 (corresponding to NMe_2 and PS-CH_2) gave final average M_n = 6.0 × 10^4 Da, PDI = 1.07. DSC (10 °C/min): T_g = 104 °C (PS) and 38 °C (PFAMS).

Synthesis and Characterization of Quaternized PS-*b*-qPFAMS Block Polyelectrolytes 7−9. A general procedure was followed for all quaternization reactions. Diisopropylethylamine (a base used to neutralize any acid residues present with the Me_2SO_4) (0.24 mL, 2.50 mmol) were added to a solution of **6** (413 mg, 6.87 mmol) in a mixture of THF (2 mL) and methanol (1 mL) at 25 °C. The reaction mixture was left stirring for 5 days. After removal of the solvent, the residue was dissolved in small amounts of THF and precipitated in hexane. Suction filtration followed by drying under high vacuum afforded the respective block polyelectrolyte **9** as amber-colored gum. Yield (230 mg, 46%). ^{1}H NMR (400 MHz, D_8 THF): δ = 0.10 (s, Si−CH_3), 1.44 (br, PS), 1.91 (s, PS), 2.59 (s, NMe_3), 2.94 (s, OSO_3−CH_3), 3.47 (s, NCH_2), 3.69−4.09 (m, Cp), 6.04−7.08 (m, Ph).

Preparation of Block Copolymer−Surfactant Complexes. A general procedure was followed to synthesize polymer−surfactant complexes. PS-*b*-qPFAMS, **9** (100 mg, 1.37 mmol), and AOT_F (77 mg, 0.11 mmol) were separately dissolved in deionized water (1 wt %) at 70 °C. Dropwise addition of the AOT_F solution to a rapidly stirring solution of the charged block copolymer at 70 °C resulted in charge neutralized material, which was further left stirring overnight. The amount of AOT_F added to block copolymer solution was strictly at 1:1 stoichiometry based on the expectation that AOT_F would be selectively complexed with quaternized amino-functionalized PFS blocks through ionic interactions. The charge-neutralized complex was then washed several times in hot deionized water (to remove any $NaMeSO_4$ salts and unreacted surfactant) and dried under vacuum (40 °C, 1 × 10^{-2} mmHg) for 30 min. These amber-colored gummy materials were then readily soluble in common organic solvents such as chloroform, THF, and toluene. Yield: 111 mg (63%). ^{1}H NMR (300 MHz, D_8 THF): δ = 0.57 (s, $SiCH_3$), 1.30−2.05 (m, PS), 2.35 (t, CH_2), 2.53 (m, CH, CH_2, NMe_3), 4.00−4.85 (m, Cp), 6.56 (m, Ph), 7.04 ppm (m, Ph). $^{19}F\{1H\}$ (282.78 MHz, D_8 THF): −81.5 (t, CF_3), −119.7 (dq, CF_2), −124.4 (dt, CF_2, −126.6 (t, CF_2). IR (see Figure S5: A characteristic change was observed in the vibrational frequency of the sulfonate group within the surfactant from 1077 cm^{-1} (AOT_F) to 1038 cm^{-1} (**9-AOT$_F$**)).

Sample Preparation of Bulk Samples and Thin Films. The preparation of bulk samples of the diblock copolymers and block copolymer−surfactant complexes was conducted by drop-casting several layers of concentrated solution of the material (50 mg/mL) from toluene to form a thick film on a glass slide. Annealing in a solvent chamber at room temperature was used as a preannealing step. Thermal annealing was performed by heating at 130 °C in vacuum for 5 days. Thermally annealed polymer samples were then analyzed using SAXS or microtomed at a thickness of ca. 60 nm and placed on a carbon-coated copper grid for TEM analysis. Thin films were deposited on a silicon wafer by spin-coating toluene solutions (10 mg/mL) for AFM analysis. The film thickness was set to between ca. 40 and ca. 200 nm by controlling the spinning rate and/or solution concentration, but all the results in this work were found to be independent of the film thickness. Spin-coated films were placed in saturated toluene vapor for 12 h for annealing.

■ ASSOCIATED CONTENT

Supporting Information. Figures S1−S5. This material is available free of charge via the Internet at http://pubs.acs.org.

AUTHOR INFORMATION

Corresponding Author

*E-mail Charl.Faul@bristol.ac.uk, Fax +44 (0)117 925 1295 (C.F.J.F.). E-mail ian.manners@bristol.ac.uk (I.M.).

ACKNOWLEDGMENT

I.M. thanks the European Union for a Marie Curie Chair, the European Research Council for an Advanced Investigator Award, and the Royal Society for a Wolfson Research Merit Award. S.K. P. thanks the European Union for a Marie Curie Postdoctoral Fellowship. C.F.J.F. thanks the University of Bristol for financial support. A special thanks to Dr. Wuge Briscoe and Georgia Pilkington for help with the SAXS experiments.

REFERENCES

(1) (a) Hamley, I. *The Physics of Block Copolymers*; Oxford Science Publications: Oxford, 1998. (b) Matsen, M. W.; Bates, F. S. *Macromolecules* **1996**, *29*, 1091–1098. (c) Bates, F. S.; Fredrickson, G. H. *Phys. Today* **1999**, *52*, 32–38. (d) Park, C.; Yoon, J.; Thomas, E. L. *Polymer* **2003**, *44*, 6725–6760.

(2) (a) Segalman, R. A. *Mater. Sci. Eng., R* **2005**, *48*, 191–226. (b) Fasolka, M. J.; Mayes, A. M. *Annu. Rev. Mater. Res.* **2001**, *31*, 323–355.

(3) (a) Kim, S. H.; Misner, M. J.; Xu, T.; Kimura, M.; Russell, T. P. *Adv. Mater.* **2004**, *16*, 226–231. (b) Cavicchi, K. A.; Berthiaume, K. J.; Russell, T. P. *Polymer* **2005**, *46*, 11635–11639.

(4) Ruokolainen, J.; Makinen, R.; Torkkeli, M.; Makela, T.; Serimaa, R.; ten Brinke, G.; Ikkala, O. *Science* **1998**, *280*, 557–560.

(5) (a) Ikkala, O.; ten Brinke, G. *Chem. Commun.* **2004**, 2131–2137. (b) Ikkala, O.; ten Brinke, G. *Science* **2002**, *295*, 2407–2409. (c) ten Brinke, G.; Ruokolainen, J.; Ikkala, O. *Adv. Polym. Sci.* **2007**, *207*, 113–177. (d) Thünemann, A. F.; Kubowicz, S.; Burger, C.; Watson, M. D.; Tchebotareva, N.; Müllen, K. *J. Am. Chem. Soc.* **2003**, *125*, 352–356.

(6) (a) Yagai, S.; Iwashima, T.; Kishikawa, K.; Nakahara, S.; Karatsu, T.; Kitamura, A. *Chem.—Eur. J.* **2006**, *12*, 3984–3994. (b) Banerjee, S.; Das, R. K.; Maitra, U. *J. Mater. Chem.* **2009**, *19*, 6649–6687. (c) Toma, H. E. *Curr. Sci.* **2008**, *95*, 1202–1225. (d) Houbenov, N.; Haataja, J. S.; Iatrou, H.; Hadjichristidis, N.; Ruokolainen, J.; Faul, C. F. J.; Ikkala, O. *Angew. Chem., Int. Ed.* **2011**, *50*, 2516–2520.

(7) Whittell, G. R.; Hager, M. D.; Schubert, U. S.; Manners, I. *Nature Mater.* **2011**, *10*, 176–188.

(8) (a) Manners, I. *Chem. Commun.* **1999**, 857–865. (b) Bellas, V.; Rehahn, M. *Angew. Chem., Int. Ed.* **2007**, *46*, 5082–5104.

(9) (a) Peter, M.; Lammertink, R. G. H.; Hempenius, M. A.; Vancso, G. J. *Langmuir* **2005**, *21*, 5115–5123. (b) Eitouni, H. B.; Balsara, N. P. *J. Am. Chem. Soc.* **2004**, *126*, 7446–7447. (c) Rider, D. A.; Winnik, M. A.; Manners, I. *Chem. Commun.* **2007**, *43*, 4483–4485. (d) Ma, Y. J.; Dong, W. F.; Hempenius, M. A.; Möhwald, H.; Vancso, G. J. *Nature Mater.* **2006**, *5*, 724–729. (e) Puzzo, D. P.; Arsenault, A. C.; Manners, I.; Ozin, G. A. *Angew. Chem., Int. Ed.* **2009**, *48*, 943–947. (f) Eloi, J.-C.; Rider, D. A.; Cambridge, G.; Whittell, G. R.; Winnik, M. A.; Manners, I. *J. Am. Chem. Soc.* **2011**, *133*, 8903–8913. (g) Shi, W.; Giannotti, M. I.; Zhang, X.; Hempenius, M. A.; Schönherr, H.; Vancso, G. J. *Angew. Chem., Int. Ed.* **2007**, *46*, 8400–8404. (h) Hempenius, M. A.; Cirmi, C.; Song, J.; Vancso, G. J. *Macromolecules* **2009**, *42*, 2324–2326. (i) Shi, W.; Cui, S.; Wang, C.; Wang, L.; Zhang, X.; Wang, X.; Wang, L. *Macromolecules* **2004**, *37*, 1839–1842.

(10) (a) Chuang, V. P.; Ross, C. A.; Gwyther, J.; Manners, I. *Adv. Mater.* **2009**, *21*, 3789–3793. (b) Chuang, V. P.; Gwyther, J.; Mickiewicz, R. A.; Manners, I.; Ross, C. A. *Nano Lett.* **2009**, *9*, 4364–4369. (c) Acikgoz, C.; Ling, X. Y.; Phang, I. Y.; Hempenius, M. A.; Reinhoudt, D. N.; Huskens, J.; Vancso, G. J. *Adv. Mater.* **2009**, *21*, 2064–2067. (d) Korczagin, I.; Lammertink, R. G. H.; Hempenius, M. A.; Golze, S.; Vancso, G. J. *Adv. Polym. Sci.* **2006**, *200*, 91–118.

(11) (a) Castruita, M.; Cervantes-Lee, F.; Mahmoud, J. S.; Zhang, Y.; Pannell, K. H. *J. Organomet. Chem.* **2001**, *637−639*, 664. (b) Paquet, C.; Cyr, P. W.; Kumacheva, E.; Manners, I. *Chem. Mater.* **2004**, *16*, 5205–5211.

(12) (a) Rider, D. A.; Liu, K.; Eloi, J. C.; Vanderark, L.; Yang, L.; Wang, J. Y.; Grozea, D.; Lu, Z. H.; Russell, T. P.; Manners, I. *ACS Nano* **2008**, *2*, 263–270. (b) MacLachlan, M. J.; Ginzburg, M.; Coombs, N.; Raju, N. P.; Greedan, J. E.; Ozin, G. A.; Manners, I. *J. Am. Chem. Soc.* **2000**, *122*, 3878–3891.

(13) (a) Hinderling, C.; Keles, Y.; Stockli, T.; Knapp, H. E.; de los Arcos, T.; Oelhafen, P.; Korczagin, I.; Hempenius, M. A.; Vancso, G. J.; Pugin, R. L.; Heinzelmann, H. *Adv. Mater.* **2004**, *16*, 876–879. (b) Lastella, S.; Jung, Y. J.; Yang, H. C.; Vajtai, R.; Ajayan, P. M.; Ryu, C. Y.; Rider, D. A.; Manners, I. *J. Mater. Chem.* **2004**, *14*, 1791–1794. (c) Lu, J. Q.; Kopley, T. E.; Moll, N.; Roitman, D.; Chamberlin, D.; Fu, Q.; Liu, J.; Russell, T. P.; Rider, D. A.; Manners, I.; Winnik, M. A. *Chem. Mater.* **2005**, *17*, 2227–2231.

(14) (a) Gädt, T.; Ieong, N. S.; Cambridge, G.; Winnik, M. A.; Manners, I. *Nature Mater.* **2009**, *8*, 144–150. (b) Xu, J. J.; Ma, Y.; Hu, W. B.; Rehahn, M.; Reiter, G. *Nature Mater.* **2009**, *8*, 348–353. (c) Wurm, F.; Hilf, S.; Frey, H. *Chem.—Eur. J.* **2009**, *15*, 9068–9077. (d) Papkov, V. S.; Gerasimov, M. V.; Dubovik, I. I.; Sharma, S.; Dementiev, V. V.; Pannell, K. H. *Macromolecules* **2000**, *33*, 7107–7115. (e) Hong, S. W.; Xu, J.; Xia, J.; Lin, Z.; Qiu, F.; Yang, Y. *Chem. Mater.* **2005**, *17*, 6223–6226.

(15) (a) Rider, D. A.; Cavicchi, K. A.; Power-Billard, K. N.; Russell, T. P.; Manners, I. *Macromolecules* **2005**, *38*, 6931–6938. (b) Lammertink, R. G. H.; Hempenius, M. A.; Thomas, E. L.; Vancso, G. J. *J. Polym. Sci., Polym. Phys.* **1999**, *37*, 1009. (c) Ramanathan, M.; Darling, S. B. *Soft Matter* **2009**, *5*, 4665–4671. (d) Rider, D. A.; Manners, I. *Polym. Rev.* **2007**, *47*, 165–195.

(16) Rulkens, R.; Ni, Y. Z.; Manners, I. *J. Am. Chem. Soc.* **1994**, *116*, 12121–12122.

(17) Wang, Z.; Masson, G.; Peiris, F. C.; Ozin, G. A.; Manners, I. *Chem.—Eur. J.* **2007**, *13*, 9372–9383.

(18) Tanabe, M.; Vandermeulen, G. W. M.; Chan, W. Y.; Cyr, P. W.; Vanderark, L.; Rider, D. A.; Manners, I. *Nature Mater.* **2006**, *5*, 467–470.

(19) Herbert, D. E.; Gilroy, J. B.; Chan, W. Y.; Chabanne, L.; Staubitz, A.; Lough, A. J.; Manners, I. *J. Am. Chem. Soc.* **2009**, *131*, 14958–14968.

(20) Gilroy, J. B.; Patra, S. K.; Mitchels, J. M.; Winnik, M. A.; Manners, I. *Angew. Chem., Int. Ed.* **2011**, *50*, 5851–5855.

(21) (a) Cheng, Z. Y.; Ren, B. Y.; Zhao, D. L.; Liu, X. X.; Tong, Z. *Macromolecules* **2009**, *42*, 2762–2766. (b) Ahmed, R.; Hsiao, M.; Matsuura, Y.; Houbenov, N.; Faul, C. F. J.; Manners, I. *Soft Matter* **2011**, *7*, 10462–10471. (c) Liu, X. H.; Bruce, D. W.; Manners, I. *Chem. Commun.* **1997**, 289–290.

(22) (a) Faul, C. F. J.; Antonietti, M. *Adv. Mater.* **2003**, *15*, 673–683. (b) Zakrevskyy, Y.; Stumpe, J.; Faul, C. F. J. *Adv. Mater.* **2006**, *18*, 2133–2136. (c) Houbenov, N.; Nykänen, A.; Iatrou, H.; Ruokolainen, J.; Hadjichristidis, N.; Faul, C. F. J.; Ikkala, I. *Adv. Funct. Mater.* **2008**, *18*, 2041–2047.

(23) Ramanathan, M.; Nettleton, E.; Darling, S. B. *Thin Solid Films* **2009**, *517*, 4474–4478.

(24) Chabanne, L.; Matas, I.; Patra, S. K.; Manners, I. *Polym. Chem.* **2011**, *2*, 2651–2660.

(25) Bates, F. S.; Fredrickson, G. H. *Annu. Rev. Phys. Chem.* **1990**, *41*, 525–557.

(26) The density (**1**) of the −fcSiMe(C≡CCH_2NMe_2)− (with a C≡CCH_2NMe_2 group on silicon) repeat unit was calculated by using the relationship $\rho = M_M/V_M$ (M_M = molar mass and V_M = molar volume) and $V_M/V_W = 1.60$ (V_W = van der Waals volume). The V_W value of PFAMS (with a C≡CCH_2NMe_2 group on silicon) was calculated by subtracting the V_W of a methyl group from the V_W value of the polyferrocenylethylmethylsilane repeating unit (V_M = 155.219 cm^3 mol^{-1}) and subsequently adding the V_W value of the C≡CCH_2NMe_2 group (tabulated by Van Krevelen) following the reference: Van Krevelen, D. W. *Properties of Polymers*, 3rd ed.; Elsevier: Amsterdam, 1990.

(27) Conventional calibration with a refractive index detector (eluent: THF containing 0.1 wt % $[Bu_4N]Br$) was required to analyze the amine-based PFS block copolymers. The role of $[Bu_4N]Br$ salt was to screen the interactions between the GPC column and the amine groups on PFAMS.

(28) Laiho, A.; Smarsly, B. M.; Faul, C. F. J.; Ikkala, O. *Adv. Funct. Mater.* **2008**, *18*, 1890–1897.

(29) The T_g of the PFAMS homopolymer is 38 °C (see Figure S2). The T_g corresponding to the PFAMS block which was not observed for the diblock materials.

(30) Smart, B. E. *Organofluorine Chemistry: Principles and Commercial Applications*; Plenum: New York, 1994.

(31) Davidock, D. A.; Hillmyer, M. A.; Lodge, T. P. *Macromolecules* **2004**, *37*, 397–407.

(32) (a) Thünemann, A. F. *Prog. Polym. Sci.* **2002**, *27*, 1473–1572. (b) Thünemann, A. F.; Lieske, A.; Paulke, B. R. *Materialwiss. Werkstofftech.* **2000**, *31*, 233–237. (c) Thünemann, A. F.; Kubowicz, S.; Pietsch, U. *Langmuir* **2000**, *16*, 8562–8567.

(33) The broad nature of the first peak may result from the synchotron beam only covering one planar direction.

(34) Duff, A. W.; Hitchcock, P. B.; Lappert, M. F.; Taylor, R. G.; Segal, J. A. *J. Organomet. Chem.* **1985**, *293*, 271–283.

(35) Downer, A.; Eastoe, J.; Pitt, A. R.; Simister, E. A.; Penfold, J. *Langmuir* **1999**, *15*, 7591–7599.